DENSE MATTER AT RHIC*

G. Roland

Massachusetts Institute of Technology
Cambridge MA 02139-4307, USA

(Received October 9, 2003)

In the first three years of running, the four RHIC experiments have collected a rich set of high quality data on nuclear collisions over a wide range in collision energy and system size. The data allow a systematic study of the evolution of the collision system from the initial state to the final freeze-out of hadrons. The measurements show convincingly that in Au+Au collisions at the highest RHIC energies, a dense, interacting medium is formed early on. In this paper, some of the key measurements are described that have revealed the unique and sometimes unexpected properties of this medium.

PACS numbers: 24.85.+p, 25.75.Nq

1. Introduction

The development of Quantum Chromodynamics (QCD) in the early 70's provided a milestone in the effort to build a complete theory of the interactions between the fundamental constituents of matter. QCD successfully describes the multitude of observed hadrons, as well as the interaction of their quark and gluon constituents at very high energies, which leads to the production of particle jets in high-energy collisions. Numerical implementations of the QCD equations, called Lattice QCD, can be used to quantitatively predict the mass-spectrum of the observed hadron states.

Still there is no analytic proof that QCD indeed describes one of the most puzzling properties of the strong interaction, the confinement of quarks and gluons inside hadrons. Despite intense experimental efforts, no free quarks have ever been observed. Lattice QCD calculations suggest that deconfinement could be achieved if strongly interacting matter were heated to a temperature of 170 MeV [1]. An example of such a calculation is can be seen in Fig. 1, which shows a phase-transition or rapid cross-over to a deconfined

* Presented at the XLIII Cracow School of Theoretical Physics, Zakopane, Poland, May 30–June 8, 2003.

state above a critical temperature. The resulting system of (almost) freely-moving quarks and gluons was termed a Quark–Gluon Plasma (QGP) [2]. This high-temperature state is believed to have existed a few microseconds after the Big Bang.

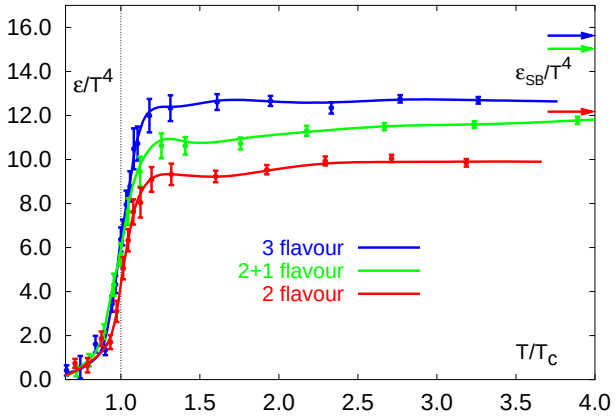

Fig. 1. Lattice QCD calculations show a phase-transition or rapid cross-over to a deconfined state of quarks and gluons at a critical temperature of $T_C \approx 170$ MeV.

In an effort to produce conditions suitable for the creation of a QGP state in the laboratory, the field of ultra-relativistic heavy-ion collisions began 18 years ago. The first studies of nuclear collisions relied on existing hadron accelerators, the Brookhaven AGS and the CERN SPS. The early experiments partially used existing detectors for particle tracking and identification. Since then the field evolved with several generations of dedicated experiments, culminating in the construction of a dedicated accelerator at BNL, the Relativistic Heavy Ion Collider (RHIC).

2. RHIC machine and experiments

The RHIC accelerator started operation in summer of 2000, after a decade of planning and construction. A detailed description of the accelerator and experiments can be found in [3]. RHIC provides collisions of Au ions at center-of-mass energy of up to 200 GeV per nucleon pair and proton–proton collisions at up to 500 GeV. The construction of the machine with two (almost) independent rings of superconducting dipole magnets also allows running with different species in each of the rings. This was crucial in the 2003 run of deuteron–gold collisions. In additions, RHIC allows collisions of polarized protons, enabling a rich spin-physics program.

Presently, collisions are provided in four interaction regions which house the four heavy-ion experiments. Two experimental collaborations, PHENIX

and STAR, operate large multi-purpose detectors, with STAR aiming for maximal coverage in single collisions and PHENIX using sophisticated triggering and particle identification to study rare observables. The smaller experiments, BRAHMS and PHOBOS, specialize in measuring hadron spectra at high rapidities and low transverse momenta respectively. PHOBOS also provides measurements of angular distributions of charged hadrons in almost the full phase-space.

In the past three years, RHIC has provided Au + Au collisions at $\sqrt{s_{NN}}$ = 19.6, 56, 130 and 200 GeV and d+Au and proton–proton collisions at 200 GeV. As the data below will demonstrate, the information from these systematic surveys, in combination with data from the AGS and CERN fixed target program, is essential in forming a consistent dynamical picture of the evolution of a heavy-ion collision.

3. QCD and heavy-ion collisions

Heavy-ion collisions provide the best opportunity to test the predictions of QCD for matter under conditions close to the QCD phase-transition and those in the early universe. However, the system created in a heavy-ion collision is different from that simulated in lattice calculations or the early universe in several important aspects. The small size of the available nuclei sets the scale of the temporal and spatial extent of the high-density system created in the collision. The asymmetry of the incoming system, with its momentum in the direction of the incoming beams, is reflected throughout the evolution of the collision. Model calculations suggest a lifetime of the collision system of 10–20 fm/c before freeze-out occurs, *i.e.* before the collision density becomes so low that the produced particles essentially enter a free-streaming motion and are finally detected by the experiments [4].

In the course of this short time, it is believed that the system evolves through a set of distinct stages, starting from an initial non-equilibrium state, where a large fraction of the incoming kinetic energy is converted into particles. In the next step, it is expected that the large particle density leads to a rapid thermalization of the system and the initial formation of a quark–gluon plasma state, over the course of a few fm/c. At the same time, the system will continue to expand longitudinally, reflecting the initial motion of the incoming nuclei, and will also develop a transverse expansion due to the large initial pressure. With a volume-doubling time of the order of a few fm/c, temperature and density will quickly fall below those necessary to sustain a deconfined partonic state and hadronization will occur. As the system continues to expand, the collision densities drop, leading to freeze-out of the particle composition ("chemical freeze-out") and momentum distributions ("kinetic freeze-out").

Obviously, the hadrons observed in the experiments, and to some extent the observed leptons and photons, are the products of this last stage of the collision after hadronization. The main experimental and theoretical challenge is then to reconstruct the properties of the earlier stages of the system from experimental observables based on these particles. In this endeavor it becomes essential to study collision systems that specifically probe the different stages of this evolution by varying the system size and collision energy. In the following, we will try to map the experimental information collected over the last 15 years onto the four stages of the collision outlined above.

3.1. Multiplicity and the initial state of the collision

One of the most basic observables in any type of high-energy collision is the multiplicity of produced charged particles, most of which are hadrons. A measurement of the angular distributions, $d^2N/d\eta d\phi$, of charged particles can be performed with a very simple detector, such as the 4-π multiplicity detector of the PHOBOS experiment. A priori, a mapping of the observed multiplicity to a specific stage of the collisions seems difficult, as in principle all stages of the collision could contribute to particle production. A close examination of the available data however suggests that the multiplicity of charged particles and the distribution in pseudo-rapidity are determined very early on in the collision and provide a window into the dynamics of the initial state.

The first multiplicity data from RHIC dealt with the charged particle pseudo-rapidity density, $dN_{\rm ch}/d\eta$, at mid-rapidity [5, 6]. Clearly, this density is related to the initial energy density of the system, as the initial volume of the system can be determined from the known size of the nuclear overlap region, in combination with an estimate of the longitudinal size at the time of equilibration, which is typically taken to be ≈ 1 fm. Early predictions for $dN_{\rm ch}/d\eta$ at RHIC, based on lower-energy nucleus–nucleus data and p+$\bar{p}$ data at $\sqrt{s} = 200$ GeV, varied by more than a factor of two [7], reflecting the uncertainty in the relative contribution of various processes in the evolution of the system. Surprisingly, the data (see Fig. 2) show that the multiplicity for central Au+Au at RHIC energies follow a smooth, approximately logarithmic evolution from lower energy collisions, which falls at the lowest end of the predictions.

In Fig. 3, data on the centrality and energy dependence of pseudo-rapidity distributions are shown [8]. It was observed that for a given centrality selection, these distributions show "limiting fragmentation". Similar to data from proton–proton collisions, all Au+Au data at large rapidities fall on a common curve, when viewed in the rest-frame of one of the colliding

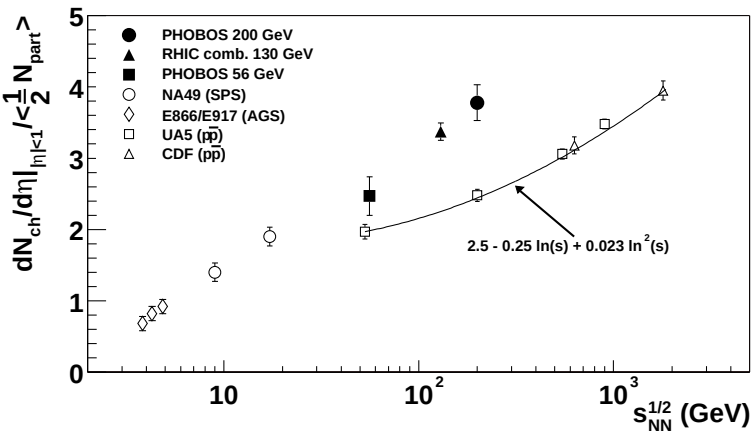

Fig. 2. Charged particle multiplicity density near mid-rapidity for central nucleus–nucleus collisions and proton–proton collisions as a function of collision energy (compilation by PHOBOS).

nuclei. Surprisingly, the shape of the pseudo-rapidity distribution for central Au+Au at $\sqrt{s_{NN}} = 200$ GeV is very similar to that in minimum bias $p + \bar{p}$ collisions and even e^+e^- collisions at the same energy [9].

It has been suggested that the relatively low multiplicity seen at RHIC is a consequence of parton saturation, based on the idea that at high energies the density of low-x gluons in the transverse plane of the colliding nuclei will no longer allow them to interact independently. Rather, they will form a "Color Glass Condensate" [10], with the resultant coherent interaction of the constituents of the nuclei limiting the growth of particle multiplicity as a function of collision energy. Model calculations based on the idea of parton saturation, in combination with local parton–hadron duality, have had impressive success in describing the energy, centrality and rapidity dependence of charged hadron production in nucleus–nucleus collisions. An example of the agreement between saturation model predictions [11] and data from BRAHMS is shown in Fig. 4 [12].

The success of the initial state saturation model, as well as the universality of the $dN/d\eta$ shapes in $p + \bar{p}$, e^+e^- and Au+Au collisions, suggests that indeed the particle multiplicity in Au+Au collisions is determined largely in the initial state of the collision and essentially remains unaltered during the evolution of the produced system. This observation also allows us to perform a first estimate of the initial energy density achieved in the collision, using data on transverse energy production from the PHENIX collaboration [13] shown in Fig. 5. Of course, defining an energy density requires that a large degree of equilibration is achieved among the produced particles, which will be discussed in the next section. Conservatively assuming an

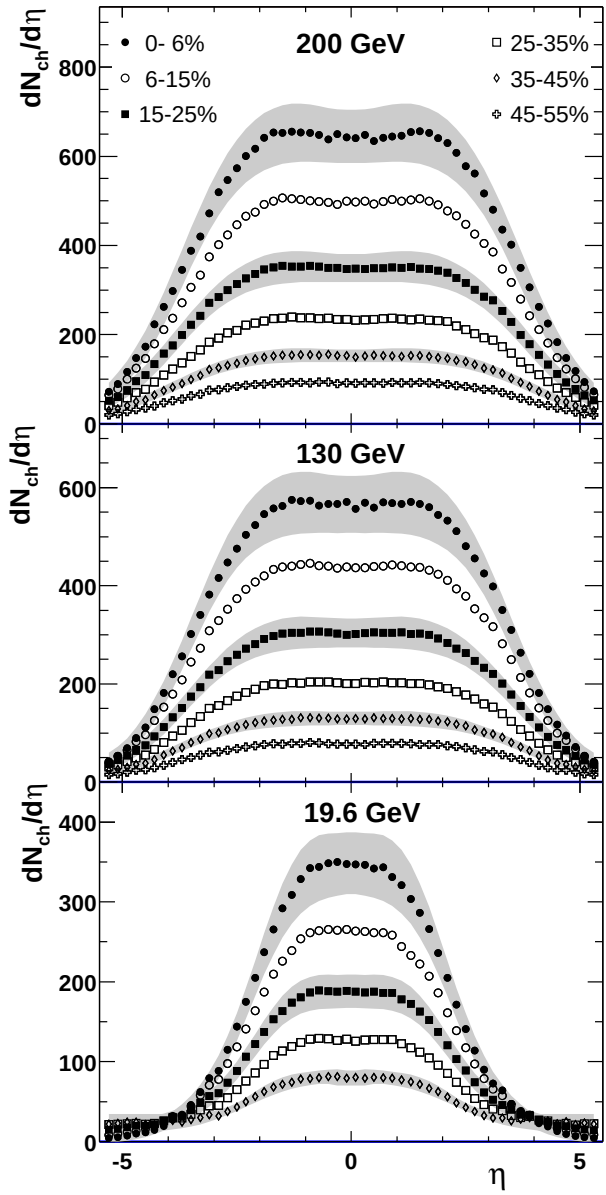

Fig. 3. Charged particle multiplicity pseudo-rapidity distributions for Au+Au collisions as a function of collision energy and centrality (PHOBOS).

equilibration time of ≈ 1 fm/c leads to an estimated initial energy density of ≈ 5 GeV/fm^3, far above the critical energy density estimated from lattice QCD calculations.

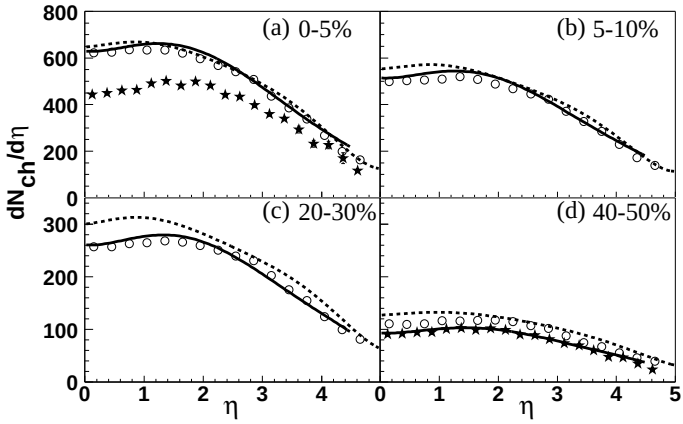

Fig. 4. Charged particle pseudo-rapidity distributions from BRAHMS for Au+Au collisions in four bins of centrality, in comparison to saturation model calculations (solid line) and the AMPT model (dashed line).

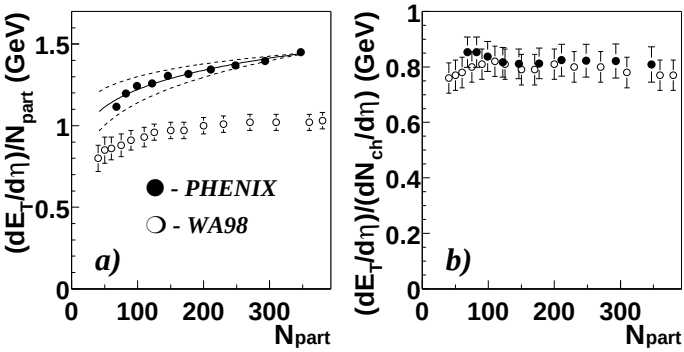

Fig. 5. Average transverse energy per charged hadron for Au+Au collisions at the CERN SPS and RHIC, measured by the WA98 and PHENIX experiments.

4. Experimental evidence for thermal equilibration

As mentioned in the previous section, it is crucial for our study of the dynamical evolution of heavy-ion collisions to understand if and at which time thermal equilibrium is achieved. It was pointed out many years ago [14] that such information can be obtained by studying the azimuthal anisotropy of the produced hadrons in nuclear collisions. Geometry shows that the initial overlap region of two nuclei for non-zero impact parameter will not be azimuthally symmetric, but rather have an American-football shape. If particle production from each individual nucleon–nucleon collision proceeded independently, this anisotropy would not be visible in the momentum dis-

tribution of the final state particles. Only if the initially produced particles rapidly form an interacting system will the configuration space anisotropy be translated into a momentum space anisotropy visible in the final state. Furthermore, as the initial anisotropy will tend to wash out without particle interaction (*i.e.* while particles are streaming freely), the study of anisotropies is also sensitive to the time at which equilibrium was achieved [4].

The first study of the final state anisotropy of charged hadron production at RHIC was performed by the STAR collaboration, shown in Fig. 6 from [15]. Here, the second Fourier-coefficient, v_2, of the azimuthal distribution of charged particles relative to the reaction plane is plotted as a function of collision centrality. The anisotropy measured by v_2 is usually referred to as "elliptic flow". As Fig. 6 shows, v_2 reaches a value bigger than 6% for the most peripheral collisions, indicating that in the direction of the reaction plane 12% more particles are emitted than perpendicular to it. The figure also shows calculations of the possible maximum value for v_2, starting from the known initial state anisotropy in configuration space and assuming a hydrodynamic expansion. Surprisingly, the data reach this so-called "hydro-limit" for mid-central collisions. This is remarkable, as the comparison to hydrodynamics implies complete local thermalization and zero mean free path of the matter constituents.

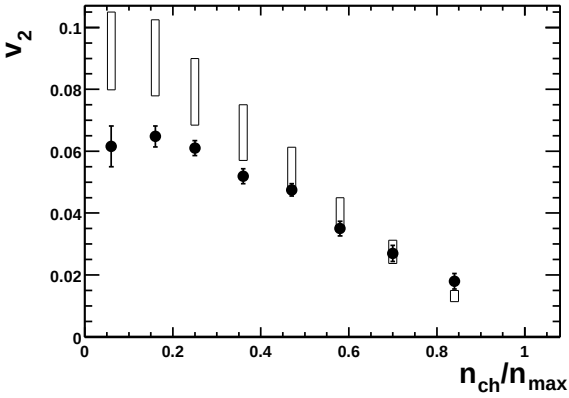

Fig. 6. Elliptic flow parameter v_2 for Au+Au collisions at 130 GeV as a function of collision centrality (STAR).

In Fig. 7, the dependence of the maximum of the v_2 parameter (averaged over p_{T}) is plotted as a function of collision energy [16]. Similar to the charged particle rapidity density, a logarithmic energy dependence of this parameter is found. Based on the arguments given above, this can be interpreted as an indication for more complete and/or earlier thermalization at the higher energies.

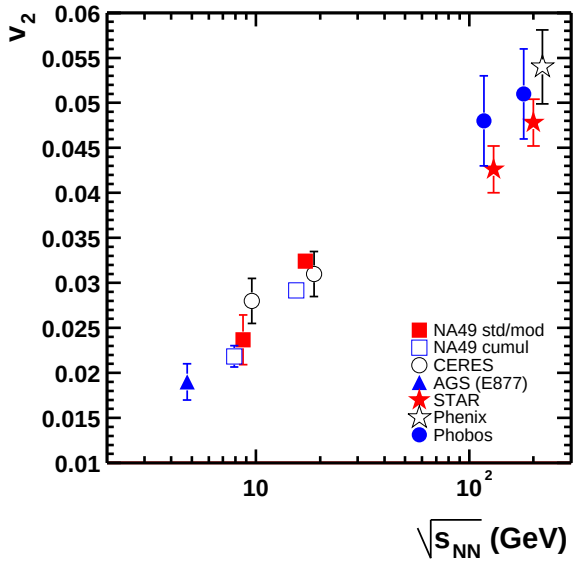

Fig. 7. Maximum of the elliptic flow parameter v_2 (averaged over p_{T}) for charged particles near mid-rapidity, as a function of collisions energy (compilation by NA49).

Since these first results, more detailed studies of the strength of elliptic flow as a function of particle mass, rapidity, and transverse momentum have been performed [17–19]. An example of such a measurement from the

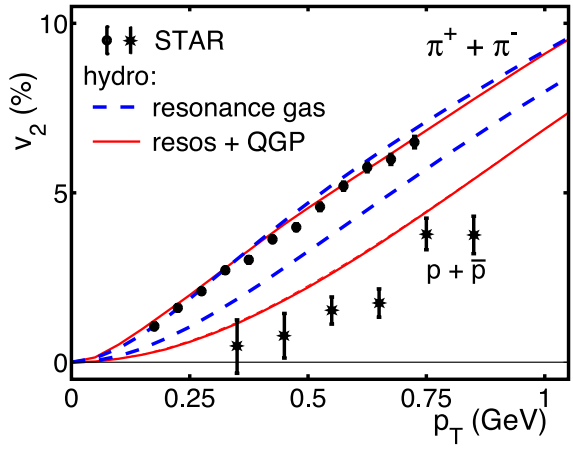

Fig. 8. Elliptic flow parameter v_2 as a function of p_{T} for pions and protons as measured by the STAR collaboration. The data are compared to calculations in a hydrodynamic model using different equations of state.

STAR collaboration is given in Fig. 8 [18], in comparison to a hydrodynamic model [4]. The data clearly show the different p_{T} dependence for particles of different mass, which is correctly predicted in hydrodynamic model calculations. The difference between dotted and solid lines indicates the sensitivity of this measurement to different equations of state. In this case, the data favor an equation of state including a phase transition to a quark–gluon plasma state.

In summary, the data on elliptic flow indicate that thermal equilibrium is indeed achieved early on in heavy-ion collisions at RHIC. Hydrodynamic calculations correctly describe the magnitude of the observed event anisotropy, as well as the mass and p_{T} dependence, in the range of $p_{\mathrm{T}} < 1$–1.5 GeV/c. The behavior at higher p_{T} will be discussed later, in the context of high p_{T} particle production.

5. Experimental evidence for chemical equilibration

Data on particle yields in heavy-ion collisions can be used to test the conditions of the particle source at chemical freeze-out. To determine the properties of the particle source at this point, statistical models are employed which describe the relative abundances of different hadron species observed in the final state using a small set of parameters. Minimally, under the assumption of complete chemical equilibration, only a freeze-out temperature and a baryo-chemical potential μ_B, which accounts for the greater density of quarks compared to antiquarks, are used in this description. It should be noted that the assumption of chemical equilibrium and importantly, also the implicit assumption that all particle ratios are defined at a common instant in the evolution of the particle source, need to be tested explicitly [20]. This requires a careful treatment of systematic errors in the available ratios data and is currently not entirely resolved. As Fig. 9 shows, however, the simplest implementation of a statistical model, with just two parameters T and μ_B, provides a very efficient description of the available data and particle abundances at RHIC for a collision energy of $\sqrt{s} = 130$ GeV [21]. Intriguingly, the resulting chemical freeze-out temperature of $T \approx 174$ MeV coincides with the critical temperature in Lattice QCD calculations. At face value, this suggests that chemical equilibrium is not achieved by hadronic interactions in the final state, but rather the hadrons are "born" into this final state by the hadronization of a high temperature partonic state [22].

It is also interesting to note that the application of the same statistical model framework to lower energy collisions and the 200 GeV RHIC data yields a smooth evolution of the freeze-out parameters, with the freeze-out temperature asymptotically approaching the value observed at RHIC.

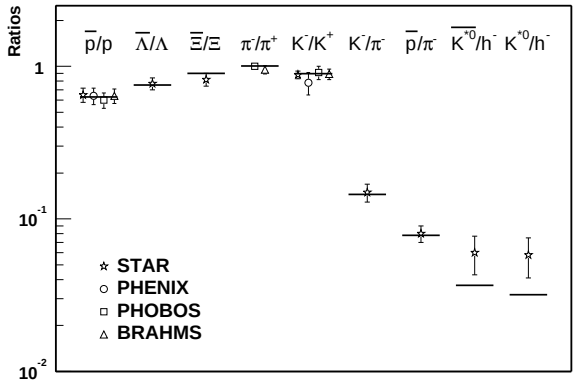

Fig. 9. Observed particle ratios in Au+Au collisions at RHIC, in comparison to calculations in a statistical model.

6. Particle production at high p_{T}

6.1. High p_{T} suppression and parton energy loss

Some of the most spectacular results at RHIC have been obtained on particle production at high p_{T} up to 10GeV/c. Particle production in this range has only become accessible in heavy-ion collisions at RHIC, due to the steep energy dependence of high p_{T} particle yields. In the theoretical analysis of particle production in hadronic and nuclear collisions, a distinction is often made between the relative contributions from "hard" parton–parton scattering processes and "soft" processes. The former can be calculated using perturbative QCD, whereas the latter are typically treated by phenomenological models that describe the non-perturbative sector of QCD [23]. The contribution from hard processes is expected to grow with increasing collision energy and to dominate particle production at high transverse momenta. Collisions of heavy nuclei offer ideal conditions to test our understanding of this picture, as "hard" processes are expected to scale with the number of binary nucleon–nucleon collisions N_{coll}, and "soft" particle production is expected to exhibit scaling with the number of participating nucleons N_{part}. For Au+Au collisions at RHIC energies, it has been predicted that the yield and momentum distribution of particles produced by hard scattering processes may be modified by "jet quenching", *i.e.* the energy loss of high momentum partons in the dense medium [24, 25]. This phenomenon has been proposed as a diagnostic tool for characterizing the parton density in the initial stage of high-energy nuclear collisions.

Indeed, the very first studies of particle production at intermediate p_{T} of 2–5 GeV/c by PHENIX showed that particle production in this p_{T} range falls far short of the expectation of binary scaling relative to nucleon–nucleon collisions, as seen in Fig. 10 for both charged hadrons and neutral pions [26].

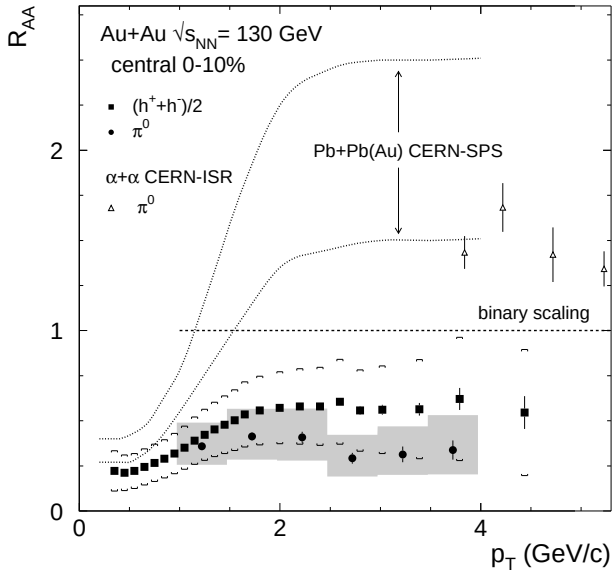

Fig. 10. Nuclear modification factor R_{AA} for charged hadrons (squares) and neutral pions (circles), as a function of transverse momentum for Au+Au collisions at $\sqrt{s} = 130$ GeV (PHENIX).

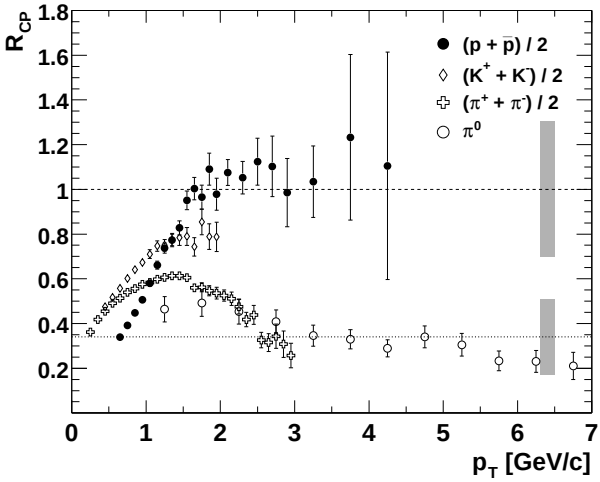

Fig. 11. Nuclear modification factor R_{AA} for charged pions, kaons and protons as a function of transverse momentum for Au+Au collisions at $\sqrt{s} = 200$ GeV (PHENIX).

This striking result has prompted a large array of measurements from all four RHIC experiments, studying particle production at intermediate and high p_{T} as a function of collision energy, collision centrality, particle mass and azimuthal angle (see *e.g.* [27–31] and references therein). An example of these measurements is shown in Fig. 11, where the nuclear modification factor R_{AA} is plotted as a function of p_{T} for charged pions, kaons and protons [32]. Interestingly, the yields for protons reach the binary scaling limit, in contrast to the large suppression of pions.

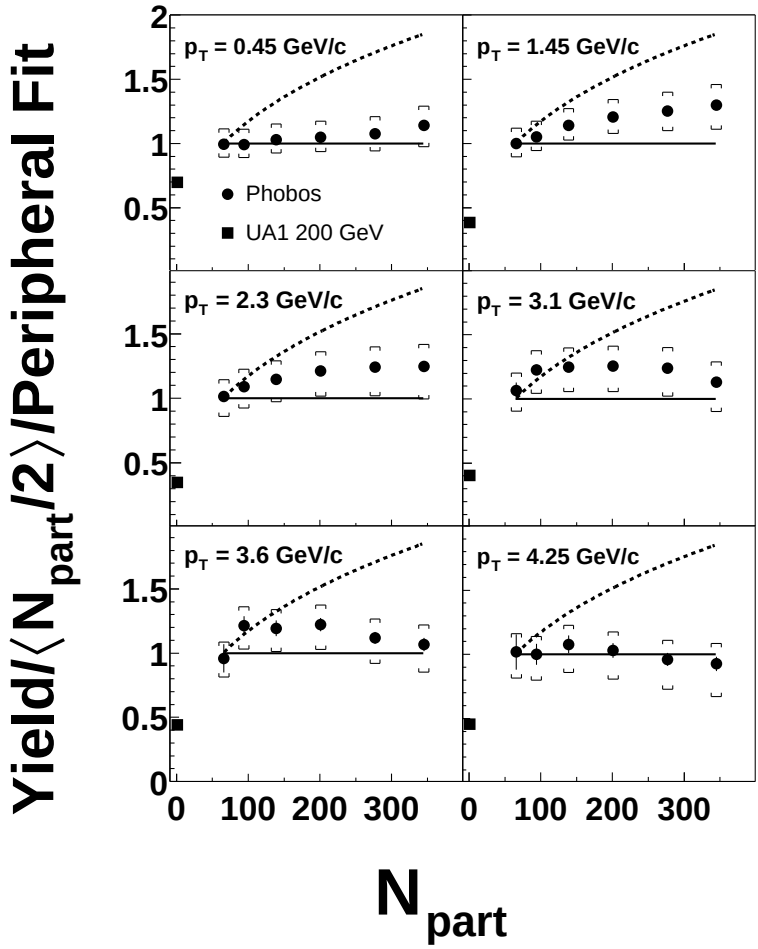

Fig. 12. Charged hadron yields per participant pair in 6 different transverse momentum bins, plotted as a function of N_{part}. The data are normalized to the yield in the most peripheral centrality bin. The dashed (solid) line shows the expectation for N_{coll} (N_{part}) scaling from semi-peripheral to central collisions.

Another intriguing result for 200 GeV Au+Au collisions is shown in Fig. 12 from the PHOBOS experiment [29], which plots the centrality dependence of charged particle yields in bins of p_{T}, starting from mid-peripheral collisions with $\approx$ 65 participating nucleons to the most central collisions. Surprisingly, one observes that charged particle yields at low p_{T} of ≈ 0.5 GeV/c and intermediate p_{T} of ≈ 4 GeV/c show a very similar centrality dependence. This leads to speculation that similar to the bulk particle production at low p_{T}, particle yields at high p_{T} could also be suppressed due to coherent effects in the initial partonic state. Indeed, calculations based on initial state effects were able to reproduce the observed magnitude of the high p_{T} suppression relative to the expectation of independent particle production [34].

In an effort to experimentally resolve the question whether the high p_{T} suppression was the result of initial state effects or the interaction of fast partons with the dense matter produced in Au+Au collisions, RHIC delivered deuteron–gold collisions. In d+Au initial state effects for the nucleons in the deuteron traversing the Au nucleus are still expected to be present,

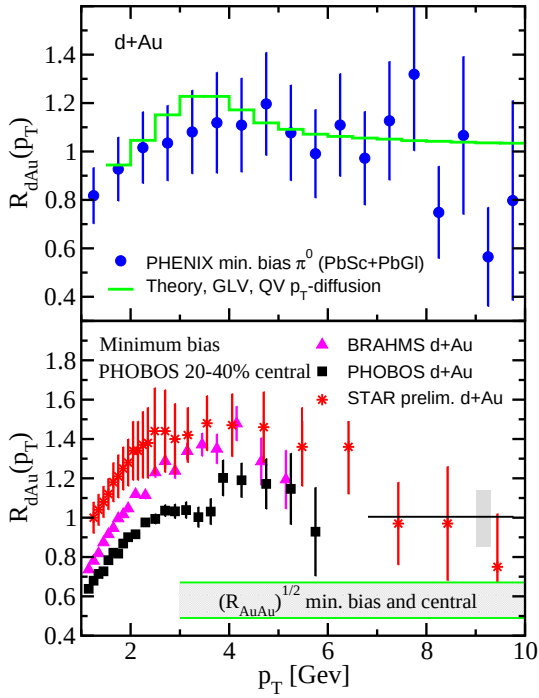

Fig. 13. Nuclear modification factor $R_{d\mathrm{Au}}$ as a function of p_{T} for d+Au collisions at $\sqrt{s} = 200$ GeV. Data are shown for neutral pions (top) and charged hadrons (bottom). The π^0 data are compared to a model calculation in the GLV formalism.

whereas no dense matter is produced and therefore no final state suppression is expected [33]. Consequently, an approach based on initial state saturation predicted a decrease in the nuclear modification factor $R_{d\mathrm{Au}}$ as a function of centrality by 25–30% [34], whereas perturbative calculations predicted an increase in $R_{d\mathrm{Au}}$ by 15% over the same centrality range [35], due to initial state p_{T} broadening.

The data on d+Au collisions [36–39] provide an unambiguous resolution to this question, as shown in Fig. 13 from [40]. Unlike in Au+Au collisions, the charged hadron and neutral pion yields reach and exceed the binary collision scaling limit, showing that the observed high p_{T} suppression is indeed connected to the presence of the dense, hot medium produced in Au+Au collisions.

This is shown impressively in Fig. 14 from STAR, where the azimuthal distribution of charged particles at high p_{T} is plotted, relative to a high p_{T} trigger particle selected for each event [36,41]. For proton+proton collisions (black circles), this distribution shows the characteristic near-side and back-

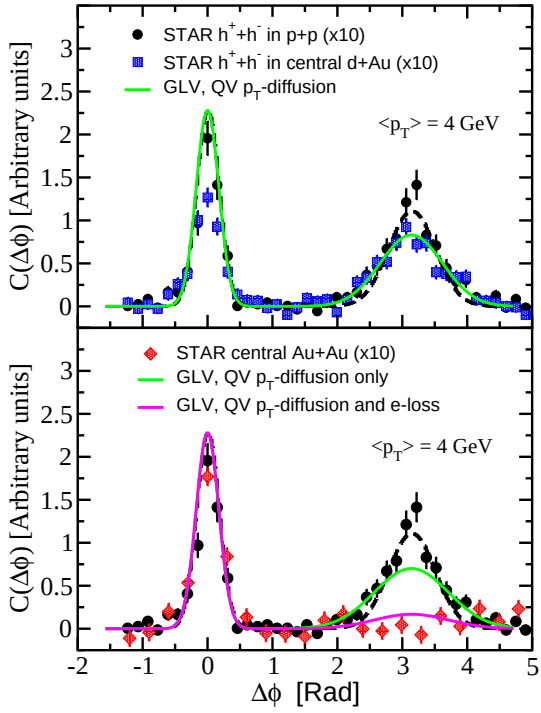

Fig. 14. Azimuthal correlations of high-p_{T} hadrons for d+Au collisions (squares, top plot) and central Au+Au collisions (diamonds, bottom), in comparison to data from p+p collisions (circles). The data are compared to a model calculation in the GLV formalism.

to-back correlation of high p_T particle jets. For Au+Au collisions (diamonds, lower plot), the near-side correlation is still present, whereas the back-to-back correlation is almost completely suppressed. This can be understood as the loss of the away-side jet due to the interaction with the medium. In d+Au collisions, both near-side and back-to-back correlations are visible, demonstrating that the loss of the away-side jet is connected to the presence of a dense medium. As Figs. 13 and 14 show, the absolute magnitude of the suppression, the lack of suppression in d+Au and the disappearance of the away-side jet in Au+Au, can be understood in a perturbative QCD model that includes the interaction of fast partons in a partonic medium [40]. The amount of suppression in this model is a measure of the gluon density, yielding values that are 30–50 times higher than in ordinary nuclear matter.

6.2. Recombination and fragmentation

One of the observations at high p_T still to be explained is the particle mass dependence of high p_T suppression and v_2. Compared to light mesons, protons and Λs show a much reduced suppression and v_2 values that exceed

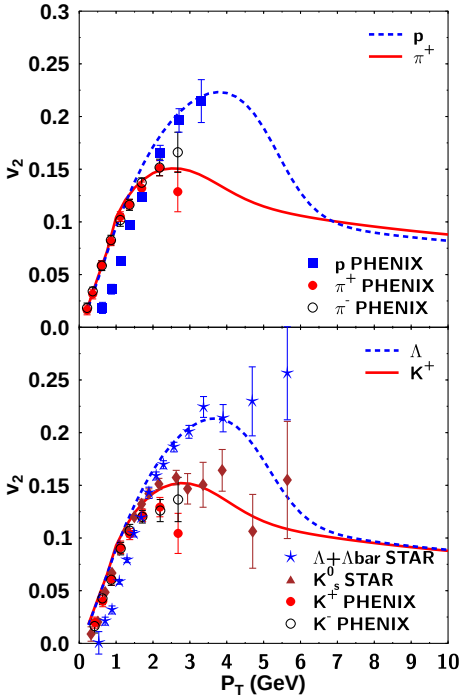

Fig. 15. Elliptic flow parameter v_2 as a function of p_T for pions, kaons, protons and Λs, in comparison to calculations in a quark recombination model.

those of mesons at high $p_{\mathrm{T}} > 2$–2.5 GeV/c. A possible resolution to this puzzle has been proposed in [42, 43] and examines the question of how hadrons are produced out of a partonic state. Calculations show [43] that for intermediate p_{T} of 1–5 GeV/c, hadron production via quark recombination from a thermalized bulk partonic state is favorable compared to hadron production from quark fragmentation as in *e.g.* jets in an e^+e^- collision. Recombination then solves both puzzles, as baryon production will be shifted to higher p_{T} relative to mesons (3 *vs* 2 quarks) and at the same time baryons will show a bigger azimuthal anisotropy when starting from the same amount of elliptic flow of the bulk partonic state. An example of this calculation for the elliptic flow of pions, kaons and Λs is shown in Fig. 15. One important consequence of this interpretation is that the observed anisotropies are directly related to the elliptic flow of the bulk partonic matter.

7. Remaining puzzles and outlook

The new data from RHIC have allowed a look at the intriguing properties of strongly interacting matter under extreme conditions. The systematics of multiplicity distributions provide a window to the very first stage of the collision, hinting at connections in particle production in apparently very different strongly interacting systems. Data on event anisotropies show that the particles produced in the initial stage rapidly form a dense, interacting system, close to (local) thermal equilibrium. Indeed, comparison to hydrodynamic calculations suggests that the system behaves almost like a liquid. That an extremely high particle density is achieved is confirmed by the studies of particle production at high transverse momenta, which show that the yields of high p_{T} hadrons escaping from the collision is only a small fraction of those based on scaling of proton–proton collisions. The study of back-to-back correlations at high p_{T} indicates that the medium formed in Au+Au collisions is opaque to fast partons. Even the most conservative estimate of the initial energy density achieved in the collision far exceeds conditions under which one could expect individual hadrons to be the constituents of the medium. Applications of quark recombination models suggest that measurements of the event anisotropy at high p_{T} may be directly probing the flow of bulk hadronic matter, driven by pressure gradients in the early collision stage.

Future studies of different collision systems and at different collision energies will allow sensitive tests of ideas and parametrizations developed to describe the present data. Additional information on the properties of the system in the initial high density phase will be provided by measurements of penetrating probes, such as real and virtual photons, which require high statistics runs planned for the upcoming running periods.

Two sets of questions will require particular attention from an experimental and theoretical side: While hydrodynamic calculations have had significant success describing single particle spectra and anisotropies at low p_{T}, they significantly overpredict the time needed for the evolution of the particle source, as shown by a comparison to two-particle correlation data in Fig. 16 [4]. Only the calculation assuming freeze-out directly at the QCD phase-transition manages to approach the data at high $k_{\perp}$. Similar observations were made for microscopic transport codes attempting to describe the correlation data. Even more importantly, no dynamical description exists so far that could explain the apparent rapid thermal and chemical equilibration suggested by the data.

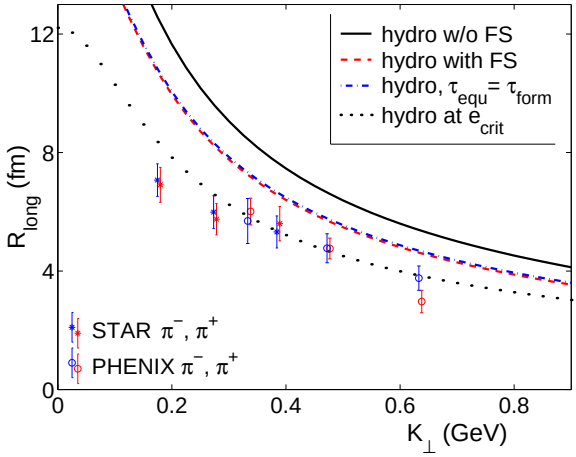

Fig. 16. R_{long}, the coherence length measured in longitudinal direction measured by two-pion Bose–Einstein correlations, as a function of pair transverse momentum $k_{\perp}$. Hydrodynamic model calculations are shown in comparison to data from STAR and PHENIX.

Equally important, further data are needed to establish if the properties of the particle source at the higher RHIC energies evolve smoothly as a function of system-size and collision energy or if a threshold behavior can be identified, over the RHIC energy range or in comparison to lower energy fixed target data.

Finally, great progress in our understanding of the new form of matter produced in heavy-ion collision is expected from the heavy-ion program at the LHC, which will provide collisions at more than order of magnitude higher energies. Correspondingly, the initial high density state at LHC will live significantly longer than at RHIC, providing a bigger window to study the workings of QCD under conditions not seen since the Big Bang.

REFERENCES

[1] See *e.g.* F. Karsch, *Nucl. Phys.* **A698**, 199 (2002).

[2] For a review, see *e.g.* B. Muller, J. Harris, *Ann. Rev. Nucl. Part. Sci.* **46**, 71 (1996).

[3] *Nucl. Instrum. Methods Phys. Res.* **A499**, 1 (2003).

[4] P. F. Kolb, U. Heinz, *Quark Gluon Plasma 3*, Eds. R.C. Hwa, X.N. Wang, World Scientific, Singapore 2003.

[5] B.B. Back *et al.*, *Phys. Rev. Lett.* **85**, 3100 (2000).

[6] B.B. Back *et al.*, *Phys. Rev. Lett.* **88**, 22302 (2002).

[7] K.J. Eskola, *Nucl. Phys.* **A698**, 78 (2002).

[8] B.B. Back *et al.*, *Phys. Rev. Lett.* **91**, 052303 (2003).

[9] B.B. Back *et al.*, `nucl-ex/0301017`, submitted to *Phys. Rev. Lett.*

[10] L.D. McLerran, R. Venugopalan, *Phys. Rev.* **D49**, 2233 (1994).

[11] D. Kharzeev, B. Levin, *Phys. Lett.* **B523**, 79 (2001).

[12] I.G. Bearden *et al.*, *Phys. Rev. Lett.* **88**, 202301 (2002).

[13] K. Adcox *et al.*, *Phys. Rev. Lett.* **87**, 052301 (2001).

[14] J.Y. Ollitrault, *Phys. Rev.* **D46**, 229 (1992).

[15] C. Adler *et al.*, *Phys. Rev. Lett.* **87**, 182301 (2001).

[16] C.A. Alt *et al.*, *Phys. Rev.* **C68**, 034903 (2003).

[17] B.B. Back *et al.*, *Phys. Rev. Lett.* **89**, 222301 (2002).

[18] C. Adler *et al.*, *Phys. Rev. Lett.* **87**, 182301 (2001).

[19] S.S. Adler *et al.*, `nucl-ex/0305013`, submitted to *Phys. Rev. Lett.*

[20] J. Rafelski, J. Letessier, *Acta Phys. Pol. B* **34**, 5791 (2003).

[21] P. Braun-Munzinger, D. Magestro, K. Redlich, J. Stachel, *Phys. Lett.* **B518**, 41 (2001).

[22] R. Stock, *Phys. Lett.* **B456**, 277 (1999).

[23] T. Sjostrand, PYTHIA manual, *Comput. Phys. Commun.* **82**, 74 (1994).

[24] M. Gyulassy, M. Plümer, *Phys. Lett.* **243**, 432 (1990).

[25] M. Gyulassy *et al.*, *Quark Gluon Plasma 3*, eds. R.C. Hwa, X.N. Wang, World Scientific, Singapore 2003.

[26] K. Adcox *et al.*, *Phys. Rev. Lett.* **88**, 022301 (2002).

[27] C. Adler *et al.*, *Phys. Rev. Lett.* **89**, 202301 (2002).

[28] K. Adcox *et al.*, *Phys. Lett.* **B561**, 82 (2003).

[29] B.B. Back *et al.*, `nucl-ex/0302015`, submitted to *Phys. Lett.* **B**.

[30] J. Adams *et al.*, `nucl-ex/0305015`, submitted to *Phys. Rev. Lett.*

[31] S.S. Adler *et al.*, `nucl-ex/0308006`, submitted to *Phys. Rev.* **C**.

[32] S.S. Adler *et al.*, `nucl-ex/0307022`, submitted to *Phys. Rev.* **C**.

[33] X.N. Wang, *Phys. Rev.* **C61**, 064910 (2000).

[34] D. Kharzeev, E. Levin, L. McLerran, *Phys. Lett.* **B561**, 93 (2003).
[35] I. Vitev, *Phys. Lett.* **B562**, 36 (2003).
[36] J. Adams *et al.*, *Phys. Rev. Lett.* **91**, 072304 (2003).
[37] S.S. Adler *et al.*, *Phys. Rev. Lett.* **91**, 072303 (2003).
[38] B.B. Back *et al.*, *Phys. Rev. Lett.* **91**, 072302 (2003).
[39] I. Arsene *et al.*, *Phys. Rev. Lett.* **91**, 072305 (2003).
[40] I. Vitev, `nucl-th/0308028`.
[41] C. Adler *et al.*, *Phys. Rev. Lett.* **90**, 082302 (2003).
[42] D. Molnar, S.A. Voloshin, *Phys. Rev. Lett.* **91**, 092301 (2003).
[43] R.J. Fries, B. Muller, C. Nonaka, S.A. Bass, `nucl-th/0306027`.
[44] P.F. Kolb, U. Heinz, *Quark Gluon Plasma 3*, Eds. R.C. Hwa, X.N. Wang, World Scientific, Singapore 2003.